Available on CMS information server **CMS CR 2003/057**

CMS Conference Report

28 November 2003

The Performance of the CMS Pixel Detector and the Primary Vertex Finding

S. Cucciarelli

University of Basle,Switzerland

on behalf od the CMS Pixel Group

Abstract

This is a template written in LaTeX, The CMS Pixel detector layout, the coverage and the hit resolution are presented. Two algorithms of primary vertex finding based on tracks reconstructed with three pixel hits are described. The primary vertex reconstruction based on pixel hits is shown to be particularly suitable for the CMS High Level Trigger.

The Performance of the CMS Pixel Detector and the Primary Vertex Finding

S. Cucciarelli, [a] on behalf of the CMS Pixel Group

[a]University of Basle, Switzerland

The CMS Pixel detector layout, the coverage and the hit resolution are presented. Two algorithms of primary vertex finding based on tracks reconstructed with three pixel hits are described. The primary vertex reconstruction based on pixel hits is shown to be particularly suitable for the CMS High Level Trigger.

1. Introduction

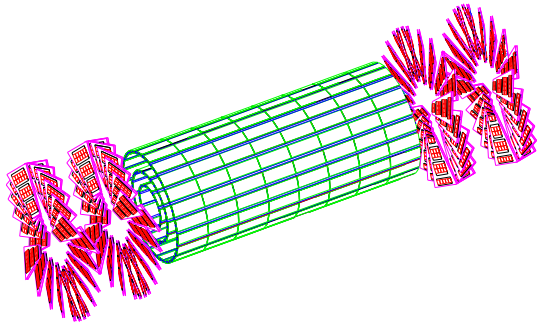

Figure 1. The Pixel detector layout.

The task of the CMS Pixel Detector is to provide high resolution three-dimensional points required for track pattern recognition and b tagging.

The Pixel detector layout considered here consists of three barrel layers with two endcap disks on each side, as shown in Figure 1. The three barrel layers are located at mean radii 4.4, 7.3 and 10.2 cm and are 53 cm long. The two disks are placed at 34.5 and 46.5 cm from the interaction point. To achieve a similarly good resolution of the vertex position in the transverse and the longitudinal planes, a design with a square pixel shape of dimensions 150×150 μm^2 and thickness 300 μm is used. To enhance the spatial resolution by analog signal interpolation the effect of charge sharing induced by the large Lorentz drift in the 4T magnetic field is used. Hence the detectors are deliberately not tilted in the barrel layers but are tilted in the end disks resulting in a turbine like geometry. The whole Pixel system consists of about 1400 detector modules arranged into half-ladders of four identical modules each in the barrel, and blades with seven different modules each in the endcaps. A more detailed description of the Pixel layout can be found in Ref. [1].

2. Pixel Detector Coverage

The pixel detector has been designed to provide two-hit coverage up to rapidity of about $\eta = 2.2$. Simulation studies show that the two-hit efficiency is close to 100 % up to $\eta \simeq 2.2$ for the "three-barrel-plus-two-disk" configuration. The full coverage up to $\eta = 2.4$ can only be achieved with an upgrade to three disks. For a stand-alone pixel track reconstruction a minimum number of three pixel hits per track are needed. This can be achieved with the three barrel layers available for the LHC high luminosity runs (10^{34} cm^{-2}s^{-1}). The 3-hit coverage is shown in Fig. 2 for the "three-barrel-plus-two-disk" configuration. The solid line shows the 3-hit efficiency as a function of the pseudorapidity when no readout losses are included. The efficiency for $\eta < 1$ is below 100 % mostly due to geometrical detector inefficiencies (there are gaps in the longitudinal direction between modules within a ladder). Detector threshold effects can also introduce some inefficiency.

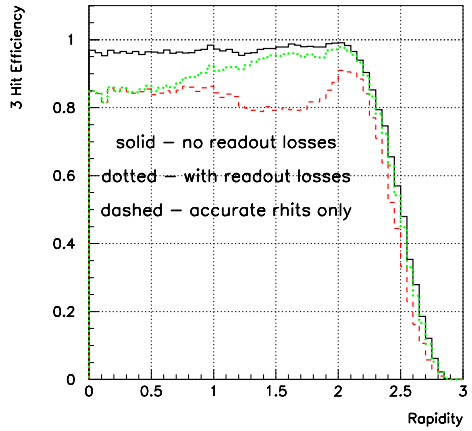

Figure 2. Three-hit efficiency as a function of the pseudorapidity for "three-barrel-plus-two-disk" configuration at high luminosity. The solid line refers to no readout losses, the dotted line includes readout losses and the dashed line considers only hit precisely reconstructed within a 100 μm window around the true position.

Although an effort was made to maximize the readout efficiency, some readout data losses will occur. Various types of readout data losses are considered in the simulation [2] depending on the CMS trigger rate, LHC luminosity and the module distance from the interaction point. The effect of readout data losses on the 3-hit coverage is described by the dotted line in Fig. 2. A loss of one or two pixels in a cluster might allow the hit position to be reconstructed, but the position is not precisely estimated. The dashed line refers to hits which survive readout losses and the position of which is within a 100 μm window around the simulated hit position. In order to reduce some of readout losses a new pixel readout chip [3] (PSI46) based on the *1/4-micron* technology has been designed and is being tested now. The new chip allows the data buffer size to be increased, which in turn reduces readout losses related to the buffer size, like the double-column time stamp buffer.

3. Hit Spatial Resolution

The CMS Pixel detector has a good position resolution in both coordinates, $\simeq 15\,\mu$m in the longitudinal barrel coordinate and $\simeq 10\,\mu$m in the $r\phi$ barrel coordinate for a 150 by 150 μm^2 square pixels and a Lorentz angle of 28°. The position resolution of the Pixel detector depends strongly on the charge sharing. In particular, in the $r\phi$ barrel direction the resolution depends on the Lorentz-induced charge sharing. Due to the radiation damage of the sensors, the Lorentz angle and the depletion depth can decrease, which results in a degradation of the position resolution. In order to prevent such a degradation the size of the new PSI46 pixel chip decreased from 150 by 150 μm^2 to 100 by 150 μm^2 (with 100 μm in the $r\phi$ direction).

The hit position reconstruction [4] is performed independently in the two directions. The prediction of the *charge width*, defined as the projection in the detector surface of the area where the charge is collected, is used in the reconstruction algorithm. If the track is partially or fully reconstructed, the impact angle to the detector is known and the charge width can be precisely evaluated, otherwise the charge width is computed assuming the track coming from (0,0,0). The last assumption provides a poor position evaluation in the longitudinal direction due to the z-coordinate uncertainty of the primary vertex (O(cm)).

To illustrate this effect in Fig. 3 the expected hit resolution is shown as a function of the charge width for the $r\phi$ barrel (x) position and clusters made of two rows, and the longitudinal barrel (y) position and clusters made of two or three columns. The top plot shows the resolution without any track information, and in the bottom plot the track direction is used to evaluate the hit position. In the y direction the knowledge of the track impact angle significantly increases the accuracy of the hit position reconstruction mostly when the charge width is much lower than the number of columns of the cluster.

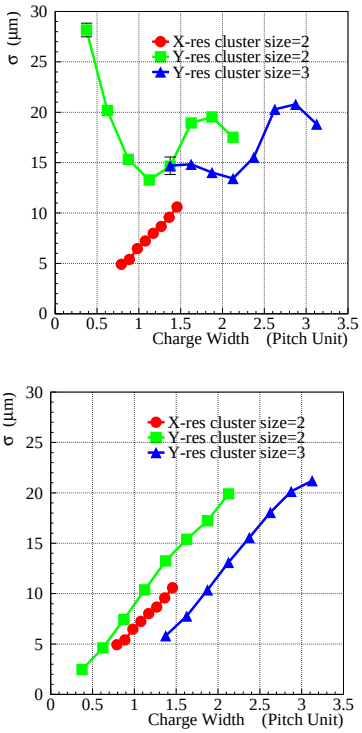

Figure 3. Expected hit position resolution as a function of the charge width for 150 by 150 μm square pixels and the Lorentz angle of 28°. The x is the $r\phi$ barrel coordinate and the y is the longitudinal barrel coordinate. In the top plot the hit position is evaluated without any track information and in the bottom one the track impact angle to the detector is used.

4. Primary Vertex Finding

The primary-vertex finding based on the pixel hits provides a simple and efficient method for the primary-vertex (PV) position measurement. This measurement is subsequently used for track seeding and in most High-Level Trigger (HLT) analyses. It must therefore be fast and precise enough. For this reason primary-vertex finding is reduced here to a one-dimensional search along the z axis. The two primary-vertex finding algorithms which are described in the following, refer to hit triplets found in the full Pixel detector acceptance. It is also possible to restrict the triplet finding to selected regions of the Pixel detector, in order to make the vertex finding faster.

The input of the PV finding algorithms consists of the relevant sets of three pixel hits (triplets) compatible with a track. The search for primary vertex along the z axis is based on the longitudinal impact point $z_{\rm IP}$ evaluation from tracks made of three hits (a more detailed description of the track parameter evaluation can be found in [5]). Figure 4 shows the $z_{\rm IP}$ resolution as a function

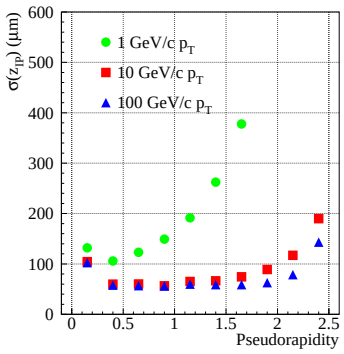

Figure 4. Resolution of the longitudinal impact point from the helix parametrization, as a function of the pseudorapidity and for for p_T values 1, 10 and 100 GeV/c.

of the pseudorapidity for single muon tracks with different transverse momenta p_T. For high p_T tracks in the barrel region the longitudinal impact point is evaluated with a resolution of $\sim 60\,\mu$m. Only pixel tracks reconstructed with p_T in excess of 1 GeV/c and a transverse impact point smaller than 1 mm are used for the vertex finding.

The output of the PV finding algorithm is a list of primary vertex candidates, denoted *PV Clusters*. Among these candidates, the *closest* primary vertex is defined as that closest in z to the simulated signal PV and the *tagged* primary vertex as that chosen by the reconstruction algorithm. For a given event, the primary vertex (tagged or closest) is *found* if it is reconstructed inside a window of 500 μm around the true PV position. The PV-finding efficiency is the frac-

tion of events with a *found* (tagged or closest) primary vertex. The closest PV-finding efficiency evaluates the ability of the algorithm to find a PV candidate. The tagged PV-finding efficiency evaluates the ability of the algorithm to identify the signal PV of the event.

4.1. Histogramming Method

The histogramming method progressively merges tracks close enough to each other in $z_{\rm IP}$, to form primary-vertex candidates. The track longitudinal impact points, $z_{\rm IP}$, are first histogrammed in 5000 bins in a $\pm 15\,$cm window around the nominal interaction point. Only the non-empty bins are kept, and their position is computed as the track $z_{\rm IP}$ weighted average. These non-empty bins are then scanned along z. A PV cluster is defined as a continuous set of consecutive bins separated by less than a certain threshold Δz. The z position of the PV cluster, $z_{\rm PV}$, is determined by averaging the $z_{\rm IP}$ of all tracks associated to this cluster. A cleaning procedure is applied to each PV cluster, rejecting the tracks distant from the PV-cluster position by more than $z_{\rm offset}$ standard deviations, i.e., such that $|z_{\rm IP} - z_{\rm PV}| < z_{\rm offset} \cdot \sigma_{z_{\rm IP}}$, where $\sigma_{z_{\rm IP}}$ is parametrized as a function of the η and p_T of the track. The z position of the PV clusters is recomputed as a weighted $z_{\rm IP}$ average of the remaining tracks.

For each PV cluster, the quantity $S = \sum p_T'^2$ is computed, where the sum runs over all the tracks associated to the cluster and

$$p'_T = \begin{cases} 0 & \text{if } p_T < p_T^{\rm min}, \\ p_T & \text{if } p_T^{\rm min} < p_T < p_T^{\rm max}, \\ p_T^{\rm max} & \text{if } p_T > p_T^{\rm max}; \end{cases} \quad (1)$$

where $p_T^{\rm min}$ is typically around $2\,{\rm GeV}/c$ and $p_T^{\rm max}$ is around $10\,{\rm GeV}/c$. The PV cluster with the largest S value is called the *tagged* PV, by definition. In the S evaluation, the tracks with a very small p_T (below $p_T^{\rm min}$) likely originating from pileup events, are not considered. A threshold is set at high momentum ($p_T^{\rm max}$) not to overweight vertices with very few high-momentum tracks, determined with a poor resolution.

Especially at high luminosity, the performance of the algorithm depends on the Δz parameter and only mildly on the $z_{\rm offset}$ parameter. Figure 5 shows the PV-finding efficiency for different values of Δz, for both the closest and tagged primary vertices. The best performance of the algorithm is reached for small values of the merging parameter due to the pollution from pileup events at high luminosity. Indeed, for large Δz values, many bins are merged together and the PV cluster is associated to many tracks either coming from other vertices or which are incorrectly reconstructed. The averaged z_{PV} value is therefore far from the true position, and the PV is subsequently not *found*.

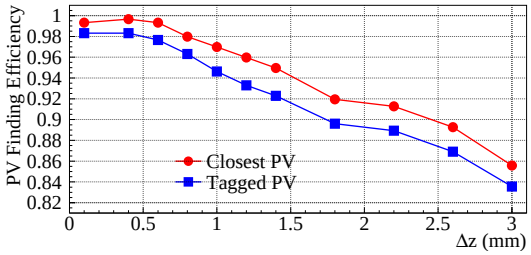

Figure 5. The PV-finding efficiency of the histogramming method. Efficiencies for the closest (circle) and tagged (square) primary vertex of the event are shown as a function of the merging parameter Δz, for high luminosity $\rm q\bar{q}$ events with E_t =100 GeV.

4.2. Divisive Method

The same set of tracks as for the histogramming method is used in the divisive method. In this method, the tracks are ordered according to increasing $z_{\rm IP}$. The ordered list is scanned to form a PV cluster until a pair of consecutive tracks separated by more than a certain threshold $z_{\rm sep}$ is found, at which point another PV cluster is built.

For each initial PV Cluster, an iterative procedure is applied to discard tracks not compatible with it. Tracks are discarded according to the $z_{\rm offset}$ parameter as explained in Section 4.1, and the cluster position is recomputed. The procedure iterates until each remaining track is declared compatible with its associated PV cluster

position. Discarded tracks are recovered to form a new PV cluster and the above procedure is applied. New PV clusters are built iteratively, until the number of remaining tracks is smaller than $N_{\rm Tk}^{\rm min}$. (Here, the choice $N_{\rm Tk}^{\rm min} = 2$ is made.) The tagged PV cluster is defined as in Section 4.1, i.e., according to the largest value of S. The performance of the divisive PV-finding in a high luminosity environment is sensitive to the value of the $z_{\rm sep}$ parameter. For large values of $z_{\rm sep}$ (above 1 mm) the closest and tagged PV-finding efficiencies decrease. In this case, it may happen that the initial PV cluster contains tracks coming from two vertices, therefore the z-PV position is between the two and most of the tracks are discarded at the next iteration. Values of the PV-finding efficiency above 95% are reached for values of the separation parameter around 500 μm or below.

4.3. Results

The two PV-finding algorithms using tracks made of three pixel hits reconstruct the z position of the primary vertex with an efficiency close to 100 % at high and low ($2{\cdot}10^{33}\,{\rm cm}^{-2}{\rm s}^{-1}$) luminosities. The PV z position is reconstructed with a resolution of about 50 μm and 40 μm at the high and low luminosity respectively and for both the histogramming and the divisive methods.

The performance comparison between the two algorithms is presented in Fig. 6, where the closest and tagged PV-finding efficiencies of both the histogramming and the divisive methods are shown for different simulated data samples at high and low luminosities. The ability of the algorithm to find a PV candidate is given by the closest PV efficiency, because the choice of the tagged PV depends also on the criterion used to order PV candidates. The divisive method gives better closest PV-finding efficiencies, while in terms of tagged PV-finding the two algorithms are comparable. Closest PV-finding efficiencies are very close to 100 % for the different samples considered here. Tagged PV-finding efficiencies are significantly below 100 % for events like $h \to \gamma\gamma$ and $B_s \to \mu\mu$, where the small average number of charged particle tracks does not allow the signal PV to be always distinguished from pileup primary vertices. Other methods to find the most likely signal PV specific to these physics channels are under investigation.

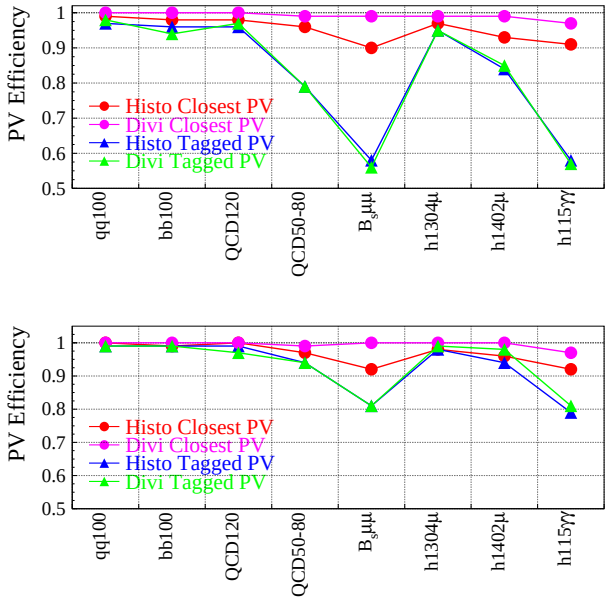

Figure 6. Tagged (circle) and Closest (triangle) PV-finding efficiencies of the histogramming and divisive methods, for different samples of simulated events at high (top) and low (bottom) luminosities.

The average time per event needed for the track parameter evaluation is about 7 ms per event. The average time for the primary-vertex finding is 0.7 ms per event, for both the histogramming and divisive methods. The time was measured on a 2.8 GHz PentiumIV and for $q\bar{q}$ events with $E_T^{\rm Jet} = 100$ GeV at high luminosity. The time quoted does not include the contributions from the hit reconstruction and the triplet finding.

5. Conclusions

Pixel hit coverage and spatial resolution have been presented. The knowledge of the impact angle of the track significantly improves the precision of the longitudinal hit position measurement.

Two primary vertex finding algorithms, the

histogramming and the divisive methods, using tracks made of three pixel hits have been developed. The divisive methods shows slightly better performance. For both the algorithms, efficiencies of primary vertex reconstruction close to 100 % are obtained for large multiplicity events, with a z-position resolution of $\sim$50 μm and $\sim$40 μm at the high and low luminosity respectively.

REFERENCES

1. The CMS Collaboration, *CMS Tracker Technical Design Report*, **CERN/LHCC 1998/06**.
2. D. Kotlinski, Nucl. Instrum. and Method **A 477** (2002) 446.
3. W. Erdmans, Proceedings of 12th International Workshop on Vertex Detectors, Nucl. Instrum. and Method **A 2004**, these proceedings.
4. S. Cucciarelli, D. Kotlinski, T. Todorov, **CMS Note 2002/049**.
5. S. Cucciarelli, M. Konecki, D. Kotlinski, T. Todorov, **CMS Note 2003/026**.